Miner Deposita (2007) 42:537–549
DOI 10.1007/s00126-007-0128-4

ARTICLE

Geochemistry of bedded barite of the Mesoproterozoic Aggeneys-Gamsberg Broken Hill-type district, South Africa

Craig R. McClung · Jens Gutzmer · Nicolas J. Beukes · Klaus Mezger · Harald Strauss · Ellen Gertloff

Received: 11 September 2006 / Accepted: 21 December 2006 / Published online: 16 February 2007

Abstract Stratiform and stratabound barite ± magnetite beds are intimately associated with the polymetallic Broken Hill-type (BHT) massive sulfide deposits of the Aggeneys-Gamsberg Pb–Zn–Cu ± Ag–Ba district in the Northern Cape Province, South Africa. Barite samples were collected and studied from four localities in the district. Although metamorphic water–rock interaction processes have partially altered the chemical and to a lesser degree the isotopic composition of barite, samples identified as being the least altered display distinctly different isotopic compositions that are thought to reflect different modes of origin. All barite samples are marked by low concentrations of SrO (0.5±0.2 wt%), highly radiogenic $^{87}Sr/^{86}Sr$ ratios, elevated $\delta^{34}S$ and $\delta^{18}O$ values compared to contemporaneous Mesoproterozoic seawater. Radiogenic $^{87}Sr/^{86}Sr$ signatures (0.7164±0.0028) point to an evolved continental crustal source for Sr and Ba, while elevated $\delta^{34}S$ values (27.3±4.9‰) indicate that contemporaneous seawater sulfate, modified by bacterial sulfate reduction, was the single most important sulfur reservoir for barite deposition. Most importantly, $\delta^{18}O$ values suggest a lower temperature of formation for the Gamsberg deposit compared with the occurrences in the Aggeneys area, i.e. Swartberg-Tank Hill and Big Syncline. The obvious differences in temperature of formation are in good agreement with the Cu-rich, Ba-poor nature of the sulfide mineralization of the Aggeneys deposits vs the Cu-poor, Ba-rich character of the Gamsberg deposit. In conjunction with this, isotopic and petrographic arguments favor a sub-seafloor replacement model for the stratabound barite occurrences of the Aggeneys deposits, while at Gamsberg, deposition at the sediment–water interface as a true sedimentary exhalite appears more likely.

Keywords Aggeneys · Gamsberg · Barite · South Africa · Broken Hill-type

Editorial handling: B. Lehmann

C. R. McClung (✉) · J. Gutzmer · N. J. Beukes · E. Gertloff
Paleoproterozoic Mineralization Research Group,
Department of Geology, University of Johannesburg,
P.O. Box 524, Auckland Park 2006,
Johannesburg, South Africa
e-mail: crmcclung@juno.com

K. Mezger
Institut für Mineralogie,
Westfälische Wilhelms-Universität Münster,
Corrensstraße 24,
48149 Münster, Germany

H. Strauss · E. Gertloff
Geologisch-Paläontologisches Institut,
Westfälische Wilhelms-Universität Münster,
Corrensstraße 24,
48149 Münster, Germany

Introduction

Sediment-hosted, stratabound, polymetallic massive sulfide deposits of the Aggeneys-Gamsberg district of the Northern Cape Province, South Africa (Fig. 1) are spatially associated with and laterally equivalent to stratiform and stratabound beds of barite ± magnetite hosted by multiply deformed and metamorphosed, amphibolite-facies metasedimentary rocks of the Mesoproterozoic Bushmanland Group (Fig. 2). The district consists of five major sulfide deposits (Swartberg, Broken Hill, Broken Hill Deeps, Big Syncline, and Gamsberg) that are regarded as typical examples of Broken Hill-type (BHT) deposits (Parr and Plimer 1993; Walters 1996). Combined, the Aggeneys-Gamsberg district had an initial estimated combined grade

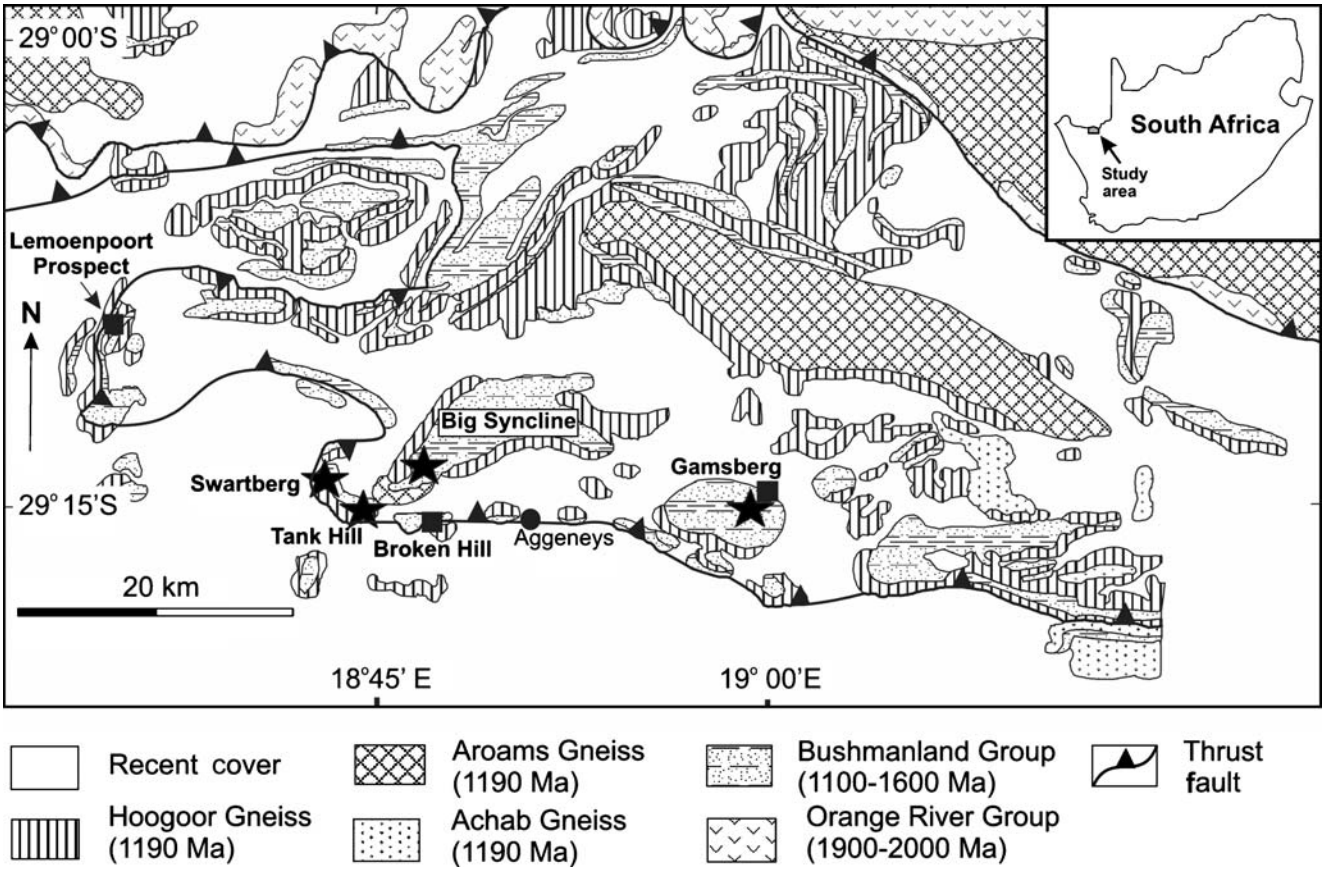

Fig. 1 Location map of the Aggeneys-Gamsberg district (after Reid et al. 1997). *Stars* denote the location of barite samples examined in this study. Absolute age constraints adapted from Bailie et al. (2005a) and McClung (2007)

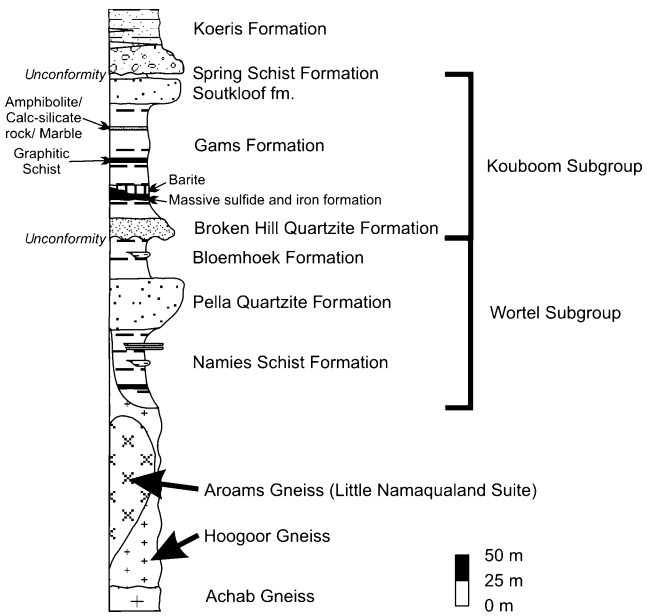

Fig. 2 Generalized stratigraphic column for the Bushmanland Group in and around the Aggeneys-Gamsberg Broken Hill-type Pb–Zn–Cu–Ag–Ba district

and tonnage of 439 Mt at 3.60% Zn, 1.43% Pb, 0.21% Cu, and 21 g/t Ag (Novak and Kihn 1994; du Toit 1998; Anglo American plc 2005), as well as an estimated 6 Mt of barite from the Gamsberg deposit (Stalder and Rozendaal 2005). The district shows a metal zonation from Pb-Zn-Cu-Ag at Swartberg in the west, to Zn-Pb-Ba at Gamsberg in the east (Table 1; Lipson 1990).

The very large Gamsberg deposit (199 Mt at 5.51% Zn; Anglo American plc 2005), in particular, is distinctly different from the Aggeneys deposits, i.e., Swartberg, Broken Hill, Broken Hill Deeps, and Big Syncline. The former is Zn dominate, with economically significant amounts of stratabound/stratiform barite that occurs stratigraphically above the laterally ore-equivalent, unmineralized pelitic schists of the Gams Formation. In contrast, the Aggeneys deposits are much smaller, Pb- and Cu-rich and associated with lower concentrations of barite.

In some sediment-hosted massive sulfide (SHMS) Pb-Zn ± Cu-Ag deposits, the accumulation of bedded barite has been identified as an integral component to the ore-forming process (Large 1983; Goodfellow et al. 1993); therefore, any constraints on barite formation may have direct implications on the formation of the spatially and geneti-

cally associated massive sulfide deposits. For the Aggeneys-Gamsberg district, in the past the genetic link between bedded barite and massive sulfide has primarily been based on the close spatial association between barite and sulfides (Rozendaal 1986; Ryan et al. 1986) and S-isotope evidence (von Gehlen et al. 1983). This communication presents the first study of bedded barite associated with the Aggeneys-Gamsberg BHT deposits, which combines three isotopic tracers, petrographic observations, and mineral chemical data. The results of this study provide new evidence that supports and expands previous genetic models for the genesis of the bedded barite and barite–magnetite occurrences (Mathias 1940; Coetzee 1958; von Gehlen et al. 1983; Barr 1988; Stalder and Rozendaal 2005).

Geological setting

The stratabound and stratiform sulfide ± barite deposits of the Aggeneys-Gamsberg district are hosted by the Mesoproterozoic Bushmanland Group, a thin (less than 1 km) multiply deformed and metamorphosed volcano-sedimentary succession (Fig. 2) located in the central Namaqua Metamorphic Complex (NMC; Joubert 1974). The NMC experienced intense polyphase deformation and medium- to high-grade metamorphism (Joubert 1971; Lipson 1978) during the Namaquan Orogeny at 1,020–1,220 Ma (Robb et al. 1999; Clifford et al. 2004). Deformation and metamorphism has been subdivided into three phases, with the first two [D_{2-3}/M_{2-3}], being the most intense. D_2 is characterized by isoclinal folding and southerly directed thrusting (Colliston and Schoch 2002) with metamorphic P-T conditions (M_2) of 630–695°C and 2.8–6 kb (Rozendaal 1975; Lipson 1978).

Because of its intensely deformed and metamorphosed nature, in combination with the difficulty in correlating between spatially distant outcrop exposures, previous authors established a series of somewhat different lithostratigraphic successions (Joubert 1974; Rozendaal 1975; Lipson 1978; Ryan et al. 1986). For the present investigation, the lithostratigraphy has been modified to incorporate the results of recent field mapping (McClung 2007) and geochronological data (Bailie et al. 2005b; McClung 2007). The base of the Bushmanland Group is intruded by an enigmatic suite of pink, leucocratic granitic gneiss (Hoogoor Gneiss), and syn- to post-tectonic S-type granites of the 1,190 Ma Little Namaqualand Suite (Bailie et al. 2005a; Fig. 2). The lower portion of the Bushmanland Group consists of an upward-coarsening succession of aluminous schists and orthoquartzites of the Wortel Subgroup. A package of dark colored quartzites, aluminous schists, and chemogenic sediments of the Kouboom Subgroup unconformably overlie the Wortel Subgroup. Metaconglomerates, psammitic schists, and ortho-amphibolites of the Koeris Formation unconformably overlie the Kouboom Subgroup and constitute the top of the Bushmanland Group.

Table 1 Summary of various characteristics of the deposits from across the Aggeneys-Gamsberg district

	West				East
	Aggeneys				Gamsberg[4, 6]
	Swartberg[1,2]	Broken Hill[3]	Broken Hill Deeps[4]	Big Syncline[5]	
Tonnage	83.2 Mt	37.9 Mt	18.8 Mt	100.0 Mt	199.3 Mt
Grade	2.52% Pb	6.35% Pb	3.98% Pb	1.01% Pb	5.51% Zn
	0.69% Zn	2.87% Zn	3.94% Zn	2.45% Zn	
	0.63% Cu	0.45% Cu	0.74% Cu	0.09% Cu	6 Mt barite
	45 g/t Ag	82 g/t Ag	56 g/t Ag	13 g/t Ag	
Host rock lithology	Oxide-/Silicate-facies IF and aluminous pelitic schist			Oxide/Silicate-facies IF and calc-silicate-rich pelitic schist	Calc-silicate-rich pelitic schist
Ore horizons	Two discrete ore horizons	Two discrete ore horizons	One discrete ore horizon	Sulfides disseminated in schist	Sulfides disseminated in schist
Barite morphology and relation to sulfides	Thin lateral equivalent	Thin lateral equivalent	Not observed	Massive body that underlies the sulfides	Massive body that overlies stratigraphically equivalent sulfide horizons
Mineralogy	Py-Po-Mag-Marc-Sph-Bar ± Gn-Cpy	Mag-Bar-Gn-Sph-Cpy-Py-Po	Mag-Sph-Gn-Cpy-Py-Po	Mag-Sph-Gn-Cpy-Py-Po ± Ba	Py-Po-Marc-Mag-Sph-Bar ± Gn-Cpy
Metal assemblage	Pb–Cu–Zn–Ag ± Ba	Pb–Zn–Cu–Ag ± Ba	Zn–Pb–Cu–Ag	Zn–Pb–Cu–Ag–Ba	Zn–Pb–Ba

Compiled from: [1] Ryan et al. (1986), [2] Anonymous (1998), [3] Du Toit (1998), [4] Anglo American plc (2005), [5] Novak and Kihn (1994), [6] Stalder and Rozendaal (2005)

IF iron formation, *Py* pyrite, *Po* pyrrhotite, *Mag* magnetite, *Marc* marcasite, *Sph* sphalerite, *Bar* barite, *Gn* galena, *Cpy* chalcopyrite

Bodies of base-metal sulfide and associated barite are restricted to the chemogenic sediments of the Kouboom Subgroup (Ryan et al. 1986; Strydom et al. 1987). The base of the Kouboom Subgroup consists of an upward-fining dark orthoquartzite of the Broken Hill Quartzite Formation. This dark orthoquartzite grades upward into pelitic schists of the Gams Formation. Locally, a thin zone of graphitic schist separates the Gams Formation into upper and lower units. The lower unit consists of an upward-fining package of aluminous schist that hosts a variably thick (0.3 to 5 m) oxide-, silicate- and carbonate-facies iron formation near the base.

Upward-coarsening aluminous schists characterize the upper unit with a single thin (1–2 m thick) amphibolite/calc-silicate rock/marble unit only developed in the west of the Aggeneys-Gamsberg district. By comparison, in the eastern portion of the Aggeneys-Gamsberg district, the upper unit of the Gams Formation comprises upward-coarsening calc-silicate-rich pelitic schists with marbles and localized beds of massive barite. An upward-coarsening orthoquartzite unit (Soutkloof Formation) gradationally overlies the schists of the Gams Formation. The top of the Kouboom Subgroup consists of upward-coarsening, aluminous schists of the Spring Schist Formation. The latter overlie the Soutkloof Formation with a sharp, but conformable contact. The Koeris Formation, a thick succession of psammitic schists, metaconglomerates and ortho-amphibolites, unconformably caps the Kouboom Subgroup.

Base-metal sulfide bodies are hosted by an oxide-/silicate-facies iron formation at the Swartberg, Broken Hill, and Broken Hill Deeps deposits, but by calc-silicate-rich pelitic schist at the Gamsberg and Big Syncline deposits (Table 1). Bedded barite is most prominent at the Gamsberg deposit (Fig. 3a), where it forms a massive bed, up to 5 m thick, and occupies a stratigraphic position immediately overlying ore-equivalent calc-silicate-rich schists in the upper portion of the Gams Formation (Fig. 4). Barite associated with the Pb- and Cu-rich ore bodies of the

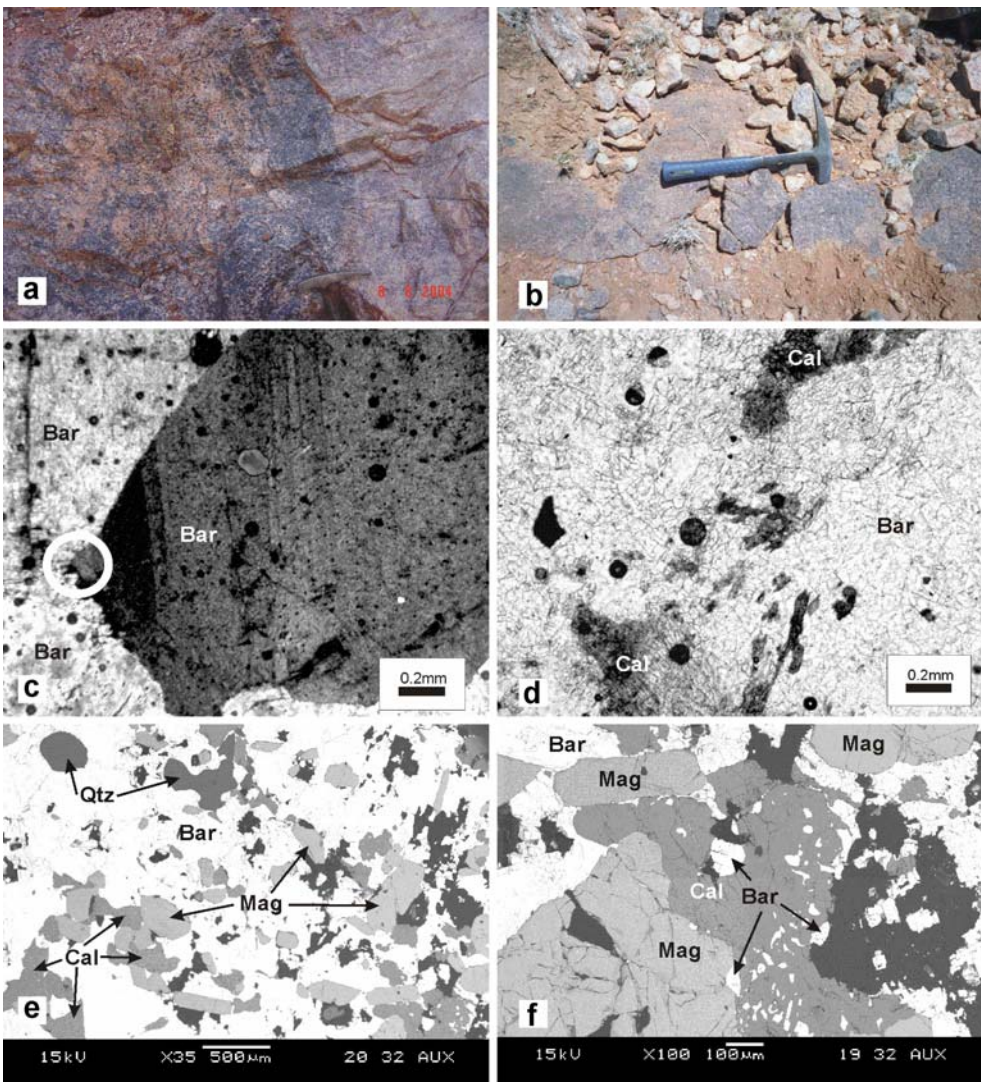

Fig. 3 **a** Photograph of interbedded massive, white, magnetite-poor to dark, magnetite-rich barite from the upper portion of the Gams Formation at Gamsberg with direction of stratigraphic younging to the *left*. Note hammer for scale. **b** Photograph of massive, dark, magnetite-rich barite from the lower portion of the Gams Formation at Tank Hill with direction of stratigraphic younging towards the *top*. Note hammer for scale. **c** Photomicrograph of Gamsberg barites in cross-polars. Note the very coarse-grained nature and triple junctions (*circle*) grain boundaries. **d** Photomicrograph of Aggeneys barite in plane transmitted light with small, irregular, brownish carbonate (calcite?) grains. **e** and **f** Back-scattered electron images of Aggeneys barite with small, irregular, calcite grains with small barite inclusions. *Cal* calcite, *Bar* barite, *Mag* magnetite, *Qtz* quartz

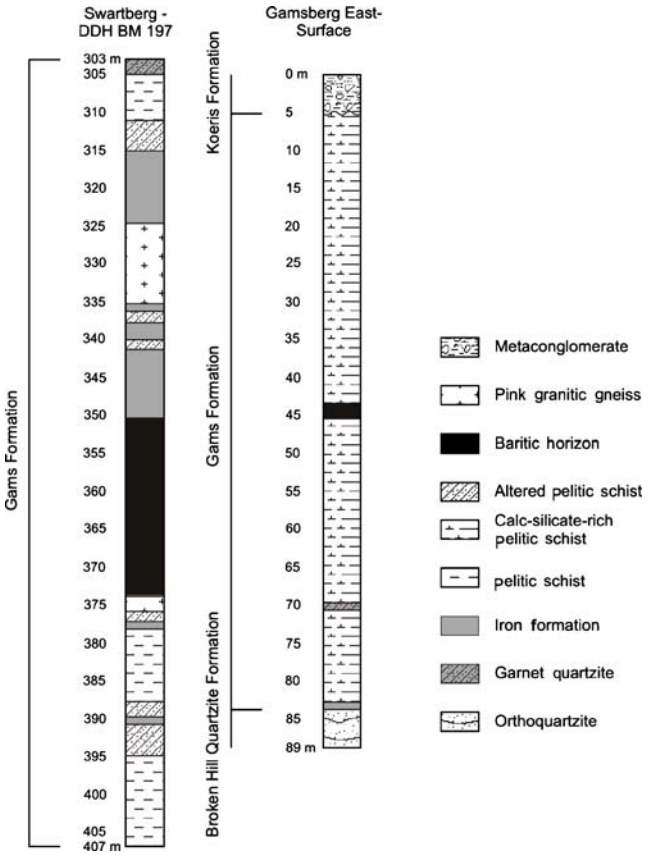

Fig. 4 Detailed section through the Gams Formation at Swartberg and Gamsberg illustrating the location of the barite beds. Note the close spatial association between the barite and iron formation at Swartberg compared to the distal relationship at Gamsberg. Note that the graphite schist was not observed in the stratigraphic section at Gamsberg

Aggeneys deposits (Table 1; Fig. 3b) occurs as a separate, but minor constituent, of the base metal sulfide bodies (Fig. 4) and can be laterally traced out into thin sulfide-free barite and magnetite–barite beds.

For this study, barite was collected from four localities: Swartberg, Tank Hill, and Big Syncline, all three in the Aggeneys area (Fig. 1), and the easternmost portion of Gamsberg. A detailed geological description of the latter occurrence was recently published by Stalder and Rozendaal (2005), where the authors documented barite–magnetite units intimately associated with a quartz-hematite lithology (i.e., oxide-facies iron formation) in the upper portion of the Gams Formation. This iron formation and associated massive barite stratigraphically overlie the pyrite-bearing ore-equivalent schists of the upper Gams Formation (Fig. 4). In contrast, stratiform and stratabound barite and barite–magnetite beds in the Swartberg-Tank Hill area occur as thin (0–20 cm thick) and 3–4 m long stratiform to stratabound lenses in a heterogeneous unit of silicified pelitic and quartz–muscovite schist, as well as garnet- and magnetite-rich quartzites of the Gams Formation. Along strike these barite–magnetite lenses grade into and alternate with lenses of magnetite-rich quartzite of a similar shape and size. Barite–magnetite beds at the Swartberg deposit were sampled from diamond drill core, where they occur interbedded with and grade laterally into laminated hematite/magnetite-garnet-quartz lithologies that are generally referred to as iron formations. These iron formations host the massive polymetallic sulfide orebodies. Stratigraphically located in the lower portion of the Gams Formation, the barite–magnetite lenses measure between 2.6–23.8 m in thickness (Fig. 4) and are considered laterally equivalent to the massive sulfide bodies (Rozendaal 1986; Ryan et al. 1986; this study). At Big Syncline (Fig. 1), lenses of barite–magnetite constitute a unit 5.7–6.5 m thick interbedded with massive amphibole and/or magnetite rock and magnetite- and garnet-rich quartzites in the lower portion of the Gams Formation. This varied succession is overlain by pyrite-bearing ore-equivalent schists of the upper Gams Formation.

Mineralogy and petrology

Bedded barite and barite–magnetite beds from all localities are coarsely crystalline (>1 cm grain size; Fig. 3c,d), with anhedral to subhedral white blocky to tabular crystals that exhibit an undulose extinction. Although volumetrically minor, some samples display clear recrystallization textures that were documented by Barr (1988). Although broadly similar in mineralogy and petrography, barite from the Aggeneys localities and the Gamsberg deposit differs in their associated mineralogy (Table 2). Magnetite and hematite

Table 2 Mineralogy of bedded barite samples from different localities in the Aggeneys-Gamsberg district

	Aggeneys			Gamsberg
	Swartberg	Tank Hill	Big Syncline	
Barite	+++	+++	+++	+++
Magnetite	+++		+++	+
Aluminosilicates	++	++	++	++
Calcite/dolomite	++		++	
Hematite	+	++		
Quartz	+	+	+	++
Muscovite	+			+
Limonite	+	+	+	+
Garnet	+		+	+
Fluorite	+		+	
Galena	+		+	
Jacobsite	+			
Rutile	+			
Sillimanite	+		+	+
Sulfosalt (?)			+	
Amphibole			+	
Apatite			+	

+++ Major (>5%), ++ Minor (<5%), + Trace (<1%)

are common minor constituents, which occur as fine disseminations within barite crystals or along foliation planes as subhedral to euhedral crystals that measure 0.5–1 mm across. In addition, minor amounts of quartz, garnet, aluminosilicate, calcite/dolomite, muscovite, and galena were identified (Table 2, Fig. 3e,f). Noteworthy is the presence of small (0.1–0.5 mm) anhedral, corroded grains of calcite/dolomite intergrown with barite at the Swartberg and Big Syncline deposits (Fig. 3e,f); such carbonate grains are absent from barite samples collected at Tank Hill and Gamsberg.

Analytical methods

Twelve barite samples were selected from outcrop and drill cores from four different localities (Fig. 1). Mineralogical and petrographical investigations were carried out using light and scanning electron microscopy on polished thin sections, as well as X-ray powder diffractometry (XRD). Powdered samples were loaded into aluminum sample holders for XRD analysis. Data were collected on a PANalytical X'pert Plus X-ray diffractometer with Cu – K_α radiation at 40 kV and 40 mA at the Central Analytical Facility (Spectrau) at the University of Johannesburg.

For geochemical analysis, the barite samples were gently crushed in an agate mortar. Magnetite was removed with a magnet, while silicate minerals were separated using bromoform and methylene iodide. The resulting barite concentrates were hand-picked under a binocular microscope until greater than 99% monomineralic.

For mineral chemical studies, polished grain mounts were prepared for 11 of the 12 barite samples at Spectrau, University of Johannesburg. Strontium concentrations in barite were measured on a CAMECA CAMEBAX 355 electron microprobe equipped with a Link eXLII energy dispersive spectrometer operated at 15 kV acceleration voltage, 10 nA sample current and 60 s counting time. Ten individual spot analyses were used to arrive at the average SrO concentration reported in Table 3. The electron microprobe analyses are reported in weight percent, with a precision of 0.3 wt% or better and a detection limit of 0.1 wt%.

Sulfur and oxygen isotope analyses were conducted at the Geologisch-Paläontologisches Institut, Westfälische Wilhelms-Universität Münster, Germany. Analysis was done in continuous-flow mode using a Carlo Erba elemental analyzer connected to a gas source Finnigan MAT DeltaPlus mass spectrometer. About 0.2 mg of finely ground barite was weighed into tin capsules for $\delta^{34}S$ analysis. To aid in the conversion of sulfur to SO_2 during combustion, V_2O_5 was added as an oxidant. For the oxygen isotope analyses, 0.2 g of ground barite was weighed into silver capsules. Barite was reduced over carbon flakes at 1,000°C to produce CO_2 and CO (Hoefs 1997). CO was then converted to CO_2 by electrical discharge between platinum electrodes (Longinelli and Craig 1967). Samples were analyzed in duplicate for sulfur isotopes and triplicate

Table 3 Mineral chemistry and isotope geochemistry for barites from the Aggeneys-Gamsberg district

	Lithology	SrO (wt%)[1]	$^{87}Sr/^{86}Sr$	$\delta^{34}S_{CTD}$ (per mil)[2]	$\delta^{18}O_{SMOW}$ (per mil)[3]
Swartberg					
BM 160E[a(cal)]	MB and GQ	0.9±0.1	0.718237±11	25.8	7.7
BM-160G[a(unk)]	MB and B	0.6±0.1	0.716088±12	26.4	7.4
BM197 CRM-A	MB	0.6±0.1	0.715987±10	20.2	6.7
BM 197 CRM-B	MB	0.6±0.1	0.716733±17	23.2	6.1
SW-BAR	MB	0.5±0.2	0.715510±10	21.5	7.2
Tank Hill					
TH-BAR	MB	0.8±0.1	0.719781±11	25.5	6.9
Big Syncline					
SW-52J	MB			34.6	6.0
SW-59E1	MB	0.5±0.1	0.716566±15	26.8	7.0
SW-59G1[a(cal)]	MM and MB	0.8±0.1	0.723110±15	25.3	4.6
SW-59G2	MB		0.719565±9	32.5	4.9
Gamsberg					
GFM-2	B	0.9±0.1			
GMDK[a(qtz)]	B	0.6±0.1	0.714842±12	34.6	14.5
GMLT[a(unk)]	B	0.8±0.1	0.715151±11	31.1	13.5

[a] Denotes samples with minute (<1%) inclusions: *cal* calcite, *qtz* quartz, *unk* unidentified inclusions;
B Massive barite, *MB* magnetite barite, *GQ* garnet quartzite, *MM* massive magnetite
[1] Each value corresponds to the average of ten spot analyses.
[2] Average of duplicate analyses
[3] Average of triplicate analyses

for oxygen isotope composition. All results are reported in delta notation relative to Canyon Diablo Troilite (VCDT) for sulfur and Standard Mean Ocean Water (VSMOW) for oxygen.

International standards as well as laboratory standards were measured to monitor the accuracy of the results. For oxygen the international standard NBS-127 was used, yielding $\delta^{18}O=9.40\pm0.03‰$ for this study. For sulfur isotope analyses the international standards IAEA-S1 (−0.3‰), IAEA-S2 (+21.55‰l), IAEA-S3 (−31.40‰) and laboratory standards CdS (+11.0‰) and AgS_2 (+2.63± 0.53‰) were used. Repeat analyses of these standard materials yielded analytical reproducibility and accuracy of 0.1‰ or better for both $\delta^{18}O$ and $\delta^{34}S$. Strontium isotope measurements were conducted at the Zentrallabor für Geochronologie, Institut für Mineralogie, Westfälische Wilhelms-Universität Münster, Germany. Strontium was separated from the matrix by standard ion-exchange procedures (AG 50W-X8 resin) on quartz glass columns using 2.5 and 6 N HCl as eluents. For mass spectrometric analysis, Sr was loaded with a TaF_5 slurry on W filaments. Isotope analyses were conducted using a Finnigan-Mat Triton multicollector mass spectrometer. Correction for mass fractionation is based on a $^{86}Sr/^{88}Sr$ ratio of 0.1194. Total procedural blanks were less than 0.15 ng for Sr. Repeat runs of NBS standard 987 gave an $^{87}Sr/^{86}Sr$ of 0.710295±0.000018.

Results

Strontium concentrations, $^{87}Sr/^{86}Sr$, $\delta^{34}S$ and $\delta^{18}O$ isotope values for barite samples are listed in Table 3 and summarized in Fig. 5. The Sr isotopic composition of barite from all occurrences examined in this study is highly radiogenic compared to estimates for contemporaneous (i.e., Mesoproterozoic) seawater at 0.7055–0.7059 (Dicken 1995) and in close agreement with primary (free of fine-grained, recrystallized barite) and muscovite-free barite samples reported in Barr (1988; Table 4). In spite of the marked differences between the $^{87}Sr/^{86}Sr$ values of barite from the Aggeneys localities (0.715510 to 0.723110) and those from the Gamsberg deposit (0.714842 and 0.715151; Fig. 5a), the samples from the Swartberg and Gamsberg deposits display a pronounced linear correlation between $^{87}Sr/^{86}Sr$ ratios and Sr concentration (Fig. 5a).

Stable isotope compositions of barite also reveal marked differences between the Gamsberg deposit and the Aggeneys localities (Table 3). Barite from the three Aggeneys localities has $\delta^{18}O$ values ranging from 4.6 to 7.7‰, compared to barite from Gamsberg with values of 13.5 and 14.5‰, respectively (Fig. 5b). The $\delta^{34}S$ values for barite from this study compare very well with data

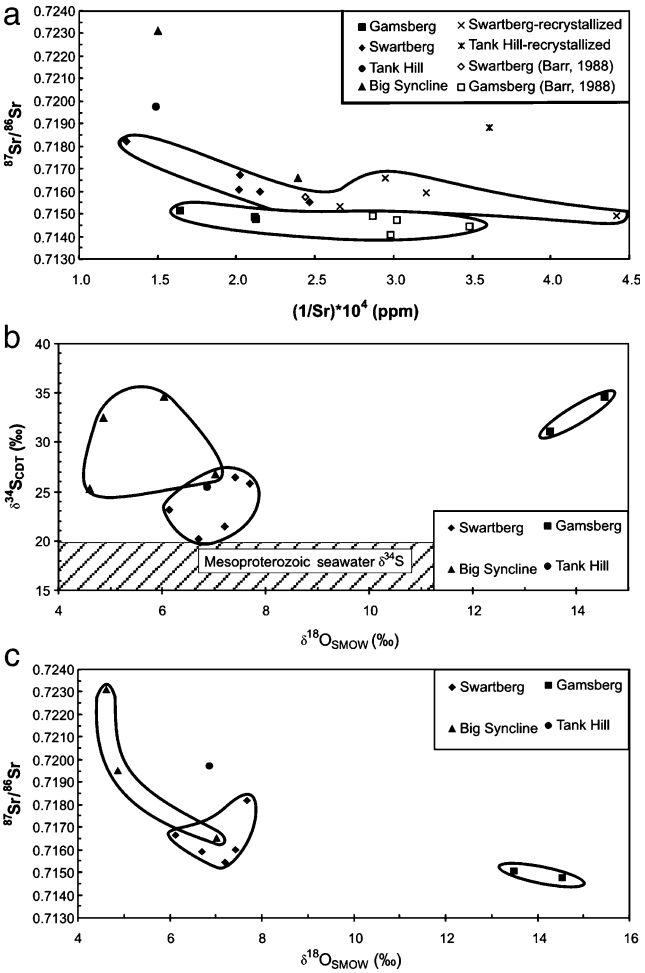

Fig. 5 Geochemistry of barite samples from the Aggeneys-Gamsberg district. **a** Plot of $^{87}Sr/^{86}Sr$ vs. the 1/Sr of barite (selected data of Barr 1988, see text; this study) illustrating possible mixing trends for barite from the Swartberg, Big Syncline, and Gamsberg deposits. *Solid symbols* represent unrecrystallized samples from this study, while *open symbols* (not recrystallized) and recrystallized samples represent data from Barr (1988). Noteworthy are those samples from Gamsberg, which show the least radiogenic signature. **b** Plot of $\delta^{18}O_{PDB}$ versus $\delta^{34}S_{CDT}$ illustrating the clear separation of the Gamsberg samples from those of the Aggeneys area. **c** Plot of $^{87}Sr/^{86}Sr$ vs the $\delta^{18}O_{PDB}$ illustrating apparent absence of correlation for Swartberg and Gamsberg. Note: Limited availability of some samples from the Big Syncline deposit only permitted analysis for all three isotope systems on two samples; see Table 3

published by von Gehlen et al. (1983). Samples for Swartberg and Tank Hill, the two westernmost localities studied, display $\delta^{34}S$ values of +20.2 to +26.4‰, distinctly lower than barite from Gamsberg (+31.1 and +34.6‰); barite from the Big Syncline deposit ranges in composition between these two end members with values between +25.3 and +34.6‰ (Table 3). This corresponds closely to the sulfide $\delta^{34}S$ values of the spatially associated massive sulfide deposits with $\delta^{34}S$ increasing from +16.0‰ at Swartberg to +29.4‰ at Gamsberg (Gertloff 2004; Table 4). Finally, sulfur and oxygen isotope values for barite from

Table 4 Compilation of available mineral chemical and isotopic data for barite and associated massive sulfides of the Aggeneys-Gamsberg district

	Sr conc. (wt%)	$^{87}Sr/^{86}Sr$	$\delta^{34}S_{CDT}$ (barite) (‰)	$\delta^{34}S_{CDT}$ (primary sulfide) (‰)[b]
Swartberg[a]	0.60±0.16[(1,2)] (n=6)	0.716383±0.000998[(1, 2)] (n=6)	23.4±2.8[(2)] (n=5)	16.0±1.6[(3)] (n=14)
Tank Hill[a]	0.80±0.10[(2)] (n=1)	0.719781±0.000011[(2)] (n=1)	25.5[(2)] (n=1)	
Broken Hill	0.32±0.10[(1)] (n=1)	0.719610±0.000006[(1)] (n=1)		17.5±2.2[(3)] (n=45)
Big Syncline	0.64±0.21[(2)] (n=2)	0.719747±0.003276[(2)] (n=3)	29.8±4.6[(2)] (n=4)	19.7±1.2[(3)] (n=15)
Gamsberg[a]	0.48±0.13[(1,2)] (n=7)	0.714703±0.000381[(1,2)] (n=7)	32.9±2.5[(2)] (n=2)	29.9±1.0[(3)] (n=23)

Results are reported as calculated means with standard deviations (1σ)
Reference: [(1)] Barr (1988); [(2)] this study; and [(3)] Gertloff (2004)
[a] Only select data of Barr (1988) used; see text for detail.
[b] Data of von Gehlen et al. (1983) omitted as only average values are reported

each locality cluster, but do not show any correlation (Fig. 5b).

Discussion

Bedded barite deposits occur in a variety of marine depositional environments. They may form as authigenic precipitates within the water column in coastal upwelling zones, diagenetically at the oxic–anoxic boundary within marine sediments, or around sites where hydrothermal fluids discharge onto the seafloor (Jewell 2000; Paytan et al. 2002). Strontium and sulfur isotopes have been successfully used to differentiate barite of different origins from modern and ancient marine successions (Paytan et al. 1993, 2002; Maynard et al. 1995; Jewell 2000). More recently, Johnson et al. (2005) illustrated that the combination of $\delta^{18}O$ and $\delta^{34}S$ data for bedded barite also provides valuable constraints on barite formation.

Preservation through metamorphism

Although barite is generally regarded as being resistant to chemical alteration (Hanor 2000; Paytan et al. 2002), it is important to assess the effects of high-grade metamorphism, such as experienced by the Bushmanland Group, on the isotopic composition of barite. It is widely known that barite is easily recrystallized during metamorphism, yet very few studies have evaluated the compositional changes that might affect barite during metamorphism (Hanor 1966 in Hanor 2000; Kříbek et al. 1996; Whitford et al. 1992). Hanor (1966 in Hanor 2000) documented a decrease in Sr concentration as a result of recrystallization during moderate- to high-grade metamorphism. Likewise, Whitford et al. (1992) pointed out that the Sr isotope ratio of barite may be altered during metamorphism if one or more of the following conditions are met: 1) very high water/rock ratios; 2) very high Sr concentration in the fluid; or 3) substantial differences between $^{87}Sr/^{86}Sr_{water}$ and $^{87}Sr/^{86}Sr_{barite}$.

Decreasing $^{87}Sr/^{86}Sr$ ratios and Sr concentrations (Fig. 5a) are correlated with increasing degrees of recrystallization (i.e., formation of small barite crystals along grain boundaries of larger grains) for the barite of the Aggeneys-Gamsberg district (see Barr 1988). Extrapolation of this trend to lower Sr and $^{87}Sr/^{86}Sr$ ratios reveals convergence of data from the Swartberg and Gamsberg deposits towards a $^{87}Sr/^{86}Sr$ value of 0.7145 (Fig. 5a). The correlation between the degree of recrystallization, lowering of the Sr concentration and decrease in $^{87}Sr/^{86}Sr$ ratio suggests that convergence on this value may have been caused by the interaction of barite with a large reservoir of metamorphic fluid with a less-radiogenic Sr-isotope signature. However, as illustrated in Fig. 5a the Sr isotopic ratio and corresponding 1/Sr do not conform to a linear array, suggesting that isotopic homogeneity was not established during metamorphism (Kříbek et al. 1996). Therefore, as isotopic equilibrium was not reached, it is likely that the barite samples displaying the least evidence for recrystallization, most radiogenic $^{87}Sr/^{86}Sr$ ratios and highest Sr concentration, retain primary or near primary isotopic values.

The $\delta^{18}O$ signature of barite can be altered by exchange with an exotic (i.e., metamorphic) fluid and/or isotopic exchange with associated oxide or silicate minerals. While the extent of the former process is difficult to assess, the latter should be reflected by homogenization of the $\delta^{18}O$ values for each locality. Such homogenization is not observed for the barite from the Aggeneys-Gamsberg district, as illustrated by the scatter of $^{87}Sr/^{86}Sr$ ratios and $\delta^{18}O$ values of samples from the Big Syncline and Swartberg deposits (Fig. 5c). However, it should be noted that while the observed scatter does preclude complete homogenization, it does not preclude some degree of re-equilibration during metamorphism and water–rock interaction. Therefore, it is assumed that the samples identified as exhibiting the least amount of alteration with respect to Sr concentrations and $^{87}Sr/^{86}Sr$ isotope ratios (i.e., GMLT, SW59-G1; BM160E and TH-BAR) are also the least affected by metamorphic re-equilibration.

Although Whelan et al. (1984) documented isotopic re-equilibration between sulfate and sulfide $\delta^{34}S$ under amphibolite-facies metamorphism, it was restricted to the scale of millimeters to centimeters. However, isotopic exchange and re-equilibration of $\delta^{34}S$ is unlikely to have been affected by metamorphism in mono-mineralic, sulfide-poor units (Kříbek et al. 1996), such as the barite beds studied here. This suggests that the $\delta^{34}S$ values of the barite samples from the Aggeneys-Gamsberg district have remained essentially unmodified by metamorphism. From the above stated, it is concluded that water–rock interaction and metamorphic recrystallization had a recognizable effect on the Sr concentration of some stratiform barite samples of the Aggeneys-Gamsberg district, but that the samples with the most radiogenic $^{87}Sr/^{86}Sr$ ratios should also display primary or near-primary $\delta^{18}O$ and $\delta^{34}S$ values that can be used in constraining the environment and mode of barite formation.

Source of barium

As the crystal structure of barite readily incorporates significant amounts of Sr (i.e., 5,000 ppm Sr), but negligible amounts of Rb (i.e., few parts per million), the Sr isotopic composition of barite generally represents the composition of the host fluid at the time of mineral formation (Hanor 2000). As discussed in the previous section, some barite samples of the Aggeneys-Gamsberg district have experienced a decrease in their Sr concentration and $^{87}Sr/^{86}Sr$ ratio during metamorphism and related water–rock interaction.

Barite samples GMLT (Gamsberg), SW59-G1 (Big Syncline), BM160E (Swartberg), and TH-BAR (Tank Hill) were identified as being the least affected by metamorphic fluid–rock interaction, as they retain the highest concentrations of Sr and the most radiogenic $^{87}Sr/^{86}Sr$ ratios. Strontium isotope ratios recorded for these samples are significantly more radiogenic than contemporaneous Mesoproterozoic seawater (0.7055–0.7059; Dicken 1995), indicating that Sr, and Ba by inference, were sourced from evolved continental crust (Whitford et al. 1992; Paytan et al. 1993, 2002; Martin et al. 1995).

Source of sulfur

While the extent to which contemporaneous seawater sulfate acts as a reservoir for marine sulfide deposits remains a subject of controversy (Goodfellow et al. 1993; Ohmoto and Goldhaber 1997; Jewell 2000), it certainly is the most important sulfur reservoir for the formation of spatially and temporally associated sulfates (Johnson et al. 2005). Sulfur isotope values recorded for the bedded barite of the Aggeneys-Gamsberg district range from +20.2 to +34.6‰, i.e., values are equivalent or significantly higher than the $\delta^{34}S$ composition of Mesoproterozoic seawater sulfate (17±3 per mil; Strauss 1993). This observation is in excellent agreement with $\delta^{34}S$ values observed for stratiform barite associated with many SHMS deposits (Fig. 6) and is attributed to the effects of concurrent microbial sulfate reduction of seawater sulfate in a closed or restricted basin (Ohmoto and Rye 1979; Hanor 2000; Jewell 2000; Johnson et al. 2005). The positive covariation of $\delta^{34}S$ values for both sulfides and sulfates between different localities in the Aggeneys-Gamsberg district suggests that sulfate and sulfide share a common source (Goodfellow et al. 1993). This further indicates that sulfur for both sulfate and sulfide was sourced from contemporaneous seawater modified by variable amounts of microbial sulfate reduction in a restricted basin.

Temperature

There is currently no reliable constraint on the $\delta^{18}O$ value for Mesoproterozoic seawater sulfate that may be used to compare the barite of the Aggeneys-Gamsberg district against. However, following the suggestion of Godderis and Veizer (2000), it may be argued that $\delta^{18}O$ of seawater was constant through time (i.e., close to 0‰). Assuming that isotopic exchange between H_2O and SO_4^{2-} reached equilibrium conditions at elevated temperatures (see Hanor 2000; Seal et al. 2000; Johnson et al. 2005), the $\delta^{18}O$ signature of barite can be used to estimate the temperature of barite precipitation. For this estimate, only $\delta^{18}O$ values of those barite samples classified as being the least affected by water–rock interaction and metamorphic re-equilibration were used.

The equations of Kusakabe and Robinson (1977) and Zheng (1999) for temperature-dependent oxygen isotope fractionation in the barite–H_2O system yields minimum temperatures of 225±30°C for the least altered barite samples from the Aggeneys localities and a minimum temperature estimate of 119±6°C for the Gamsberg deposit. The latter estimate is unreliable because isotopic exchange between H_2O and sulfate becomes effective only at temperatures above 150°C (Hanor 2000; Seal et al. 2000; Johnson et al. 2005). However, this estimate does suggest a much lower temperature of barite precipitation at the Gamsberg deposit, compared to the Aggeneys localities.

Origin of bedded barite

The formation of stratabound and stratiform barite deposits in marine successions requires the mixing of at least two fluids, one sulfate-poor and thus capable of transporting significant amounts of Ba and Sr, and the second sulfate-bearing (Jewell 2000). Isotopic and mineral chemical data

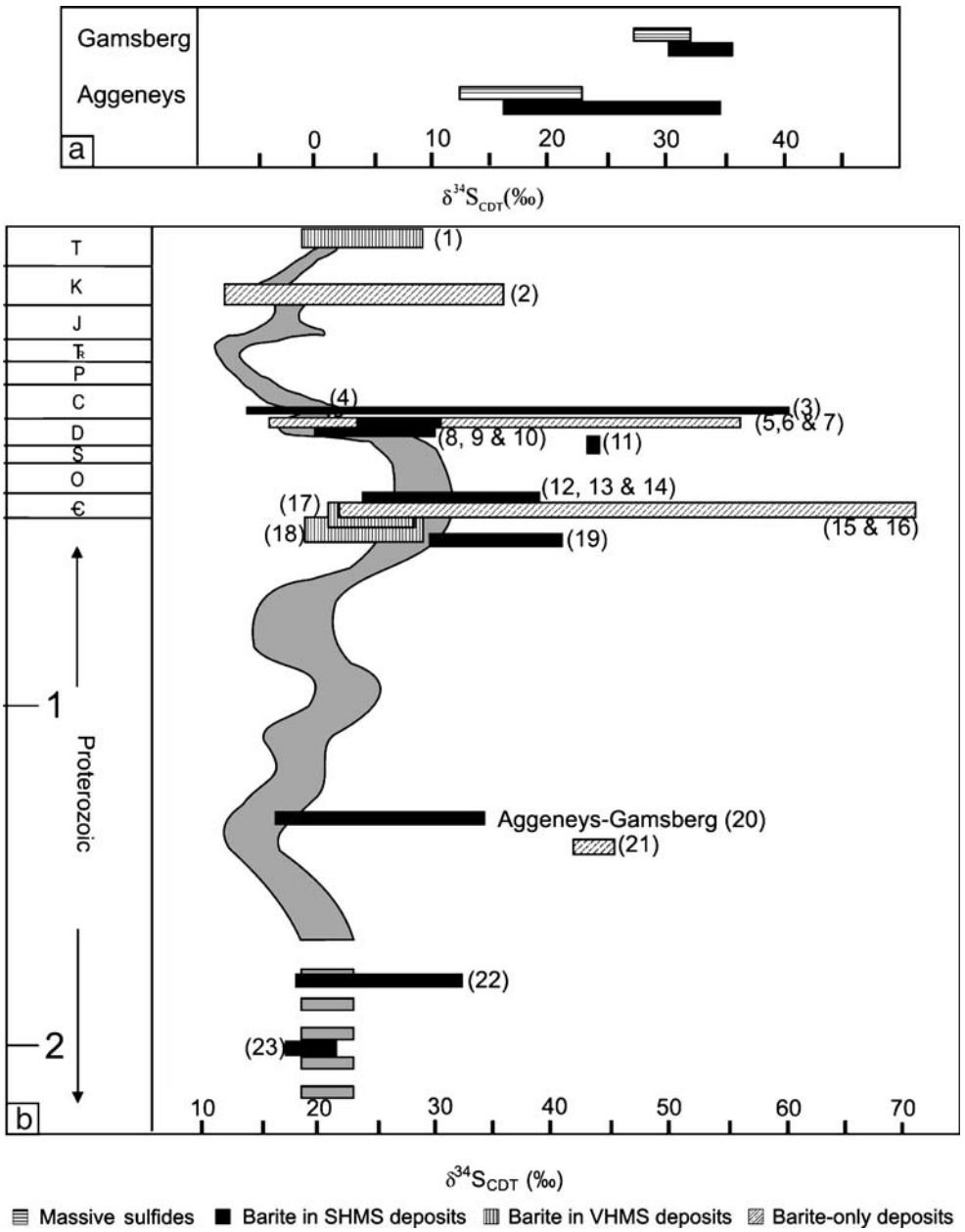

Fig. 6 **a** Comparison of $\delta^{34}S$ values for barite and massive sulfide samples (von Gehlen et al. 1983; Gertloff 2004; this study) from the Gamsberg and Aggeneys deposits, respectively. **b** Comparison of $\delta^{34}S$ values for barite from Aggeneys-Gamsberg with SHMS deposits, volcanic-hosted (VHMS) deposits, marine barite deposits, and the marine S-isotope curve. Data obtained from compilations by Maynard et al. (1995), Jewell (2000), and Clark et al. (2004) unless noted otherwise. Marine sulfur isotope curve modified from Claypool et al. (1980) and Strauss (1993). (1) Kuroko, (2) Mexico, (3) Red Dog (Johnson et al. 2005), (4) Arkansas, (5) Chaudfontaine, (6) Nevada, (7) Lower Earn Group, (8) Meggen, (9) Rammelsberg, (10) Jason, (11) Vulcan, (12) Faro, (13) Grum, (14) Dy, (15) Qinling Region, (16) Jiangnan Region, (17) Barite Hills, (18) Roná (Kříbek et al. 1996), (19) Aberfeldy, (20) Aggeneys-Gamsberg (von Gehlen et al. 1983; Gertloff 2004; this study), (21) Mangampeta, (21) McArthur River (Strauss 1993), and (23) Jagat (Deb et al. 1991)

for barite of the Aggeneys-Gamsberg district have allowed for identification of these fluids as contemporaneous Mesoproterozoic seawater and a crustal hydrothermal fluid.

Sulfur and oxygen isotope values acquired for barite from the Aggeneys-Gamsberg district define distinct clusters for each locality (Fig. 5b), with higher sulfur and oxygen isotope values for barite from Gamsberg, compared to the other localities. The clustering of sulfur and oxygen isotope values of barite from the Aggeneys-Gamsberg district closely matches observations by Johnson et al. (2005) for bedded barite from the giant Red Dog SHMS deposit of Alaska. Similarities include the lack of correlation between oxygen and sulfur isotope values, as well as a distinct but limited increase in $\delta^{34}S$ from contemporaneous seawater sulfate. Based on these and other observations, Johnson et al. (2005) identified contemporaneous seawater sulfate as the major sulfur source, with microbial sulfate reduction in a restricted reservoir responsible for the elevated $\delta^{34}S$ values. Although the model of Johnson et al. (2005) has been adopted here, it is acknowledged that both kinetic isotope fractionation during microbial sulfate reduction (higher O-isotope values) and sulfate–H_2O isotopic exchange reactions at temperatures >150°C are required to account for the observed variations in the $\delta^{18}O$ values of the sulfates.

Barite of the Aggeneys localities is intimately associated with Cu-rich massive sulfide ore bodies that appear to replace a ferruginous (i.e., iron formation) protolith (Mathias 1940; McClung 2007). Oxygen isotope values

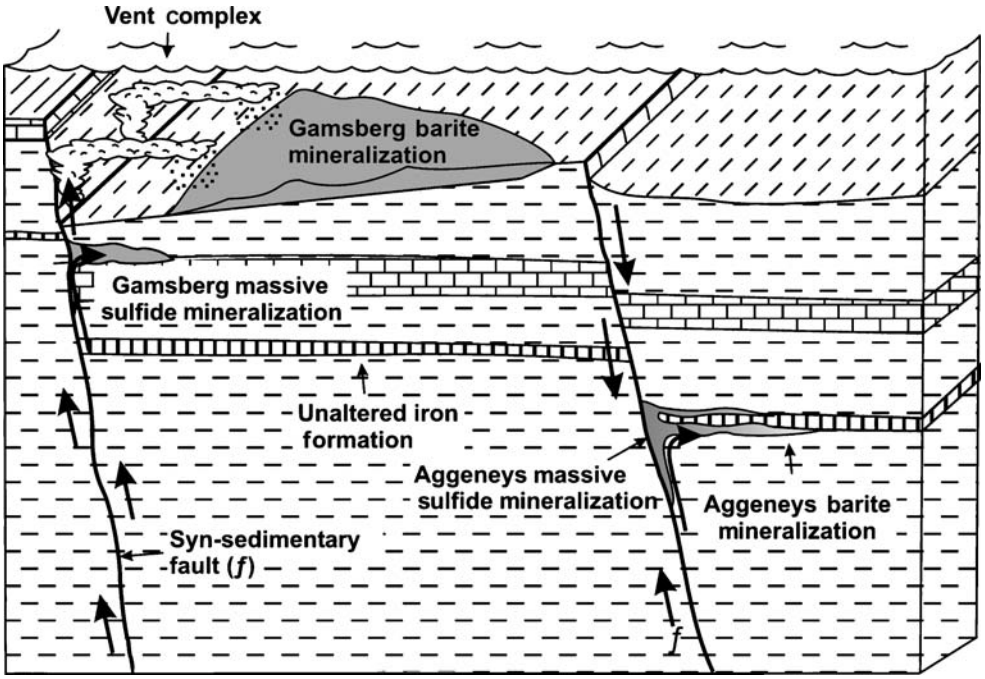

Fig. 7 Schematic diagram illustrating the formation of stratiform and stratabound barite and associated massive sulfides via sub-seafloor replacement of an iron-formation in the Aggeneys deposits, and seafloor exhalation in the Gamsberg deposit. Both deposit styles are related to mixing of an upwelling metalliferous hydrothermal fluid and downward moving sulfate-rich seawater. Modified from Robb (2005)

for these stratabound, replacive barite occurrences suggest temperatures of formation in excess of 250°C. This corresponds well with temperatures necessary for hydrothermal fluids to leach and transport significant amounts of Cu (see Hannington et al. 1999). It is, therefore, proposed that the bedded barite and barite–magnetite occurrences at Aggeneys formed in a sub-seafloor environment where metal-bearing, hydrothermal fluids mixed with sulfate-rich pore waters from a restricted basin.

Conversely, the bedded barite of the Gamsberg deposit occurs distal to the massive sulfide bodies. Oxygen isotope values suggest distinctly lower temperatures of barite formation compared with occurrences in the Aggeneys area. There is no evidence for a replacive origin for this barite and deposition at the seafloor, i.e., a syn-sedimentary environment, is likely. $\delta^{34}S$ values for barite from the Gamsberg deposit as high as +35‰ suggest a marine sulfate reservoir efficiently depleted in ^{32}S by bacterial sulfate reduction (BSR). Therefore, exhalation of a low temperature (100–200°C), Ba-rich, hydrothermal fluid into a small, restricted sedimentary basin appears the most likely scenario for barite formation at the Gamsberg deposit.

Conclusions

Although stratiform and stratabound barite occurrences from the Aggeneys-Gamsberg district have been partially affected by amphibolite-facies metamorphism and associated water–rock alteration, a detailed evaluation of their petrography, mineral chemistry, and isotopic systematics yields strong evidence that barite formed in environments commonly associated with sediment-hosted massive sulfide (SHMS) deposits. Barite associated with the Cu-rich, Ba-poor polymetallic, massive sulfide orebodies of the Aggeneys deposits is thought to have formed through subseafloor replacement of a pre-existing iron formation through mixing of contemporaneous Mesoproterozoic seawater with a relatively hot (>250°C) hydrothermal fluid. In contrast, barite at the Cu-poor, Ba-rich Gamsberg deposit, appears to have formed at a lower temperature as synsedimentary exhalative mineralization distal to sulfide deposition (Fig. 7).

Acknowledgments The authors greatly acknowledge permission by Anglo American plc. to publish these results. This work was supported by grants from Anglo American Exploration Division, the National Research Foundation of South Africa, and the Technology and Human Resources for Industry Program (THRIP) to NJB and by the Society of Economic Geologists to CRM. H. Baier (Zentrallabor für Geochronologie, Institut für Mineralogie, Westfälische Wilhelms-Universität Münster) is thanked for conducting Sr isotope analyses and A. Fugmann (Geologisch-Paläontologisches Institut, Westfälische Wilhelms-Universität Münster, Germany) for providing O- and S-isotope data on the barite samples. We would also like to thank Bernd Lehmann and several anonymous reviewers who critically reviewed previous versions of this manuscript.

References

Anglo American plc (2005) Anglo American creating long term shareholder value. Annual Report, 127 pp

Anonymous (1998) Anglo to develop Gamsberg. Mining Journal, September 11, pp 193

Bailie RH, Armstrong RA, Reid DL (2005a) Age and composition of the granitic gneisses of the Aggeneys district, Namaqua Province, South Africa. Geo2005, University of KwaZulu-Natal, Durban, 4–7 July, pp 7

Bailie RH, Armstrong RA, Reid DL (2005b) Geochronology of the Bushmanland Group, Aggeneys, Namaqua Province, South Africa. Geo2005, University of KwaZulu-Natal, Durban, 4–7 July, pp 9

Barr JM (1988) Isotope character of barite and ore genesis in Central Bushmanland. unpublished masters thesis, Johannesburg, University of Witwatersrand, 208 pp

Clark SHB, Poole FG, Zhongcheng W (2004) Comparison of some sediment-hosted, stratiform barite deposits in China, the United States, and India. Ore Geol Rev 24:85–101

Claypool GE, Holser WT, Kaplan IR, Sakai H, Zak I (1980) The age curves of sulfur and oxygen isotopes in marine sulfate and their mutual interpretation. Chem Geol 28:199–260

Clifford TN, Barton ES, Stern RA, Duchesne J-C (2004) U–Pb zircon calendar Namaquan (Grenville) crustal events in the granulite-facies terrane of the O'okiep copper district of South Africa. J Petrol 45:669–691

Coetzee CB (1958) Manganiferous iron ore, hematite, barite, and sillimanite on gams (portion 1), Namaqualand. Geological Survey of South Africa Bulletin 28:1–29

Colliston WP, Schoch AE (2002) The structural development of the Aggeneys Hills, Namaqua Metamorphic Complex. S Afr J Geol 105:301–324

Deb M, Hoefs J, Baumann A (1991) Isotopic composition of two Precambrian stratiform barite deposits from the Indian shield. Geochim Cosmochim Acta 55:303–308

Dicken AP (1995) Radiogenic isotope geology. Cambridge University Press, Cambridge, pp 503

Du Toit MC (1998) Lead. In: Wilson MGC, Anhaeusser CR (eds) The mineral resources of South Africa. Council for Geosciences, Pretoria, pp 424–432

Gertloff EC (2004) Petrology and sulfur isotope geochemistry of the metamorphosed Cu-Pb-Zn-Ag deposits of the Aggeneys-Gamsberg district, Bushmanland, South Africa. unpublished diploma thesis, Münster, Westfälische Wilhelms-Universität, 104 pp

Godderis Y, Veizer J (2000) Tectonic control of chemical and isotopic composition of ancient oceans; the impact of continental growth. Am J Sci 300:434–461

Goodfellow WD, Lydon JW, Turner RJW (1993) Geology and genesis of stratiform sediment-hosted (SEDEX) zinc-lead-silver sulfide deposits. In: Kirkham RV, Sinclair WD, Thorpe RI, Duke JM (eds) Mineral deposit modeling. Geological Association of Canada Special Paper 40:201–251

Hannington MD, Bleeker W, Kjarsgaard I (1999) Sulfide mineralogy, geochemistry, and ore genesis of the Kidd Creek deposit: part I. north, central, and south orebodies. Econ Geol Monogr 10:163–224

Hanor JS (1966) The origin of barite. unpublished doctoral thesis, Cambridge, Harvard University, 257 pp

Hanor JS (2000) Barite-celestine geochemistry and environments of formation. In: Alpers CN, Jambor JL, Nordstrom DK (eds) Sulfate minerals—crystallography, geochemistry and environmental significance. Reviews in Mineralogy and Geochemistry, Mineralogical Society of America, 40, pp 193–276

Hoefs J (1997) Stable isotope geochemistry, 4th edn. Springer, Berlin Heidelberg New York, pp 201

Jewell PW (2000) Bedded barite in the geological record, in marine authigenesis: from global to microbial. Society of Economic Paleontologist and Mineralogists Special Publication 66, pp 147–161

Johnson CA, Kelley KD, Leach DL (2005) Sulfur and oxygen isotopes in barite deposits of the Western Brooks range, Alaska, and implications for the origin of the Red Dog massive sulfide deposits. Econ Geol 99:1435–1448

Joubert P (1971) The regional tectonism of the genesis of part of Namaqualand. Precambrian Research Unit Bulletin, Cape Town, University of Cape Town 10:1–210

Joubert P (1974) Geologic map of Aggeneys-Pofadder area. Precambrian Research Unit, Cape Town, University of Cape Town, 1:100,000, 1 sheet

Kříbek B, Hladíková J, Žák K, Bendl J, Pudilová M, Uhlík Z (1996) Barite–hyalophane sulfide ores at Roná, Bohemian Massif, Czech Republic: metamorphosed black shale-hosted submarine exhalative mineralization. Econ Geol 91:14–35

Kusakabe M, Robinson BW (1977) Oxygen and sulfur isotope equilibria in the $BaSO_4$-H_2SO_4–H_2O system from 110° to 350°C and application. Geochim Cosmochim Acta 41:1033–1040

Large DE (1983) Sediment-hosted massive sulphide lead-zinc deposits: an empirical model. In: Sangster DF (ed) Sediment-hosted stratiform lead–zinc deposits. Mineralogical Association of Canada Short Course Handbook 8, pp 1–29

Lipson RD (1978) Some aspects of the geology of part of the Aggeneysberge and surrounding gneisses, Namaqualand. unpublished masters thesis, Johannesburg, University of Witwatersrand, 100 pp

Lipson RD (1990) Lithogeochemistry and origin of metasediments hosting the Broken Hill deposit, Aggeneys, South Africa, and implications for ore genesis. unpublished doctoral thesis, Cape Town, University of Cape Town, 250 pp

Longinelli A, Craig H (1967) Oxygen-18 variations in sulfate ions in sea-water and saline lakes. Science 156:56–59

Martin EE, MacDougall JD, Herbert TD, Paytan A, Kastner M (1995) Strontium and neodymium isotopic analysis of marine barite separates. Geochim Cosmochim Acta 59:1353–1361

Mathias M (1940) The occurrence of barite in an iron ore deposit in Namaqualand. Trans R Soc S Afr 28:207–217

Maynard JB, Morton J, Valdes-Nodarse EL, Diaz-Carmona A (1995) Sr isotopes of bedded barites: guide to distinguishing basins with Pb–Zn mineralization. Econ Geol 90:2058–2064

McClung CR (2007) Basin analysis of the Mesoproterozoic Bushmanland Group of the Namaqua Province, South Africa. unpublished doctoral thesis, Johannesburg, University of Johannesburg, pp 317

Novak D, Kihn C (1994) The base metal deposits of Aggeneys, Northern Cape. unpublished company report, Black Mountain Mine Ltd

Ohmoto H, Goldhaber MB (1997) Sulfur and carbon isotopes. In: Barnes HL (ed) Geochemistry of hydrothermal ore deposits, 3rd edn. Wiley, New York, pp 517–612

Ohmoto H, Rye RO (1979) Isotopes of sulfur and carbon. In: Barnes HL (ed) The geochemistry of hydrothermal ore deposits. Wiley Interscience, New York, pp 509–561

Parr JM, Plimer IR (1993) Models for Broken Hill-type lead-zinc-silver deposits. In: Kirkham RV, Sinclair WD, Thorpe RI, Duke JM (eds) Mineral deposit modeling. Geological Association of Canada Special Paper 40, pp 253–288

Paytan A, Kastner M, Martin EE, MacDougall JD, Herbert T (1993) Marine barites as a monitor of seawater strontium isotope composition. Nature 366:445–449

Paytan A, Mearon S, Cobb K, Kastner M (2002) Origin of marine barite deposits: Sr and S isotope characterization. Geology 30:747–750

Reid DL, Smith CB, Watkeys MK, Welke MK, Betton PJ (1997) Whole-rock radiometric age patterns in the Aggeneys-Gamsberg ore district, Central Bushmanland, South Africa. S Afr J Geol 100:11–22

Robb L (2005) Introduction to ore-forming processes. Blackwell, Oxford, p 373

Robb LJ, Armstrong RA, Waters DJ (1999) The history of granulite-facies metamorphism and crustal growth from single zircon U–

Pb geochronology: Namaqualand, South Africa. J Petrol 40:1747–1770

Rozendaal A (1975) The geology of Gamsberg, Namaqualand, South Africa. Unpublished masters thesis, Stellenbosch, University of Stellenbosch, 109 p

Rozendaal A (1986) The Gamsberg zinc deposit, Namaqualand District. In: Anhaeusser CR, Maske S (eds) Mineral deposits of Southern Africa. Geological Society of South Africa, Johannesburg, pp 1477–1488

Ryan PJ, Lawrence AL, Lipson RD, Moore JM, Paterson A, Stedman DP, van Zyl D (1986) The Aggeneys base metal sulphide deposits Namaqualand, South Africa. In :Anhaeusser CR, Maske S (eds) Mineral deposits of Southern Africa. Geological Society of South Africa, Johannesburg, pp 1447–1473

Seal RS, Alpers CN, Rye RO (2000) Stable isotope systematics of sulfate minerals. In: Alpers CN, Jambor JL, Nordstrom DK (eds) Sulfate minerals—crystallography, geochemistry and environmental significance. Reviews in Mineralogy and Geochemistry, Mineralogical Society of America 40:193–276

Stalder M, Rozendaal A (2005) Petrographic and geochemical characteristics of the Gamsberg barite deposit and its relationship to Broken Hill-type Zn-Pb mineralization. S Afr J Geol 108:35–50

Strauss H (1993) The sulfur isotopic record of Precambrian sulfates; new data and a critical evaluation of the existing record. Precambrian Res 63:225–246

Strydom D, van der Westhuizen WA, Schoch AE (1987) The iron-formations of Bushmanland in the North-Western Cape Province, South Africa. In: Uitterdijk Appel PW, LaBerge GL (eds) Precambrian Iron-formations. Theophrastus, Athens, pp 621–634

Von Gehlen K, Nielsen H, Chunnett I, Rozendaal A (1983) Sulfur isotopes in metamorphosed Precambrian Fe-Pb-Zn-Cu sulfides and barite at Aggeneys and Gamsberg. Mineralogical Magazine, South Africa, 47:481–486

Walters SJ (1996) An overview of Broken Hill type deposits. In: Pongratz J, Davidson G (eds) New developments in Broken Hill type deposits. CODES Special Publication 1, Hobart, University of Tasmania, pp 1–10

Whelan JF, Rye RO, Delorraine WF (1984) The Balmat-Edwards zinc-lead deposit: synsedimentary ore from Mississippi Valley-type fluids. Econ Geol 74:239–265

Whitford DJ, Korsch MJ, Solomon M (1992) Strontium isotope studies of barites: implications for the origin of base metal mineralization in Tasmania. Econ Geol 87:953–959

Zheng YF (1999) Oxygen isotope fractionation in carbonate and sulfate minerals. Geochem J 33:109–126